

Mechanism-based pharmacodynamic modelling of bacterial growth inhibition by antibiotics



Christoph Hethey

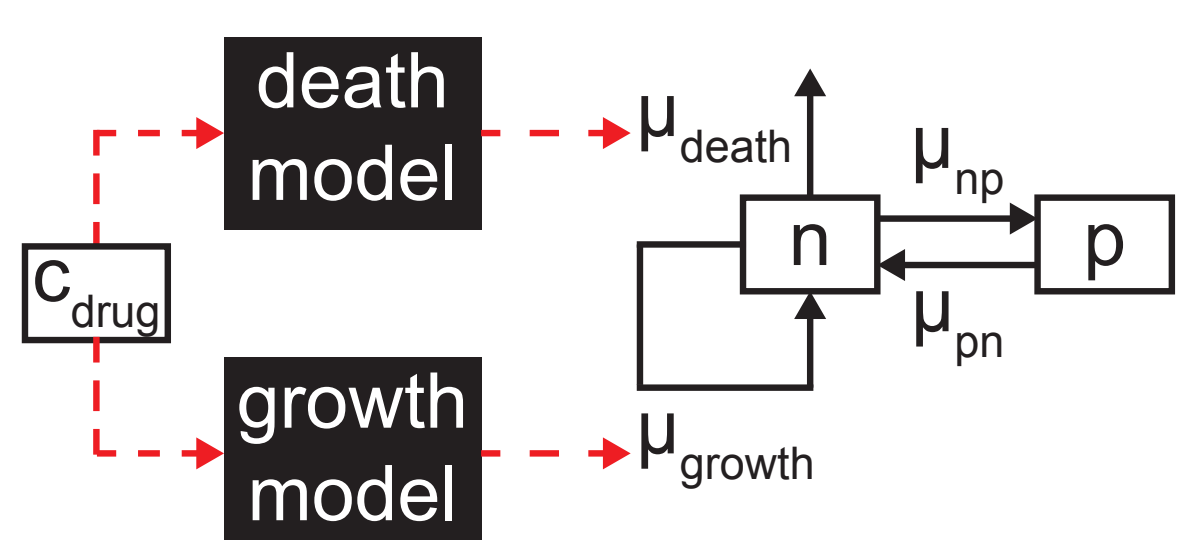
(Graduate Research Training Program PharMetX, Institut für Biochemie und Biologie, Universität Potsdam),
Charlotte Kloft (Institute of Pharmacy, Freie Universität Berlin),
Wilhelm Huisinga (Institut für Mathematik, Universität Potsdam)



Objective

Typical drug-effect models directly link exposure to antibiotics to bacterial population growth. They rarely account for known mechanisms of action of the drug — which are particularly relevant for the analysis of synergistic or antagonistic effects of drug combinations. Our aim was to develop a generic pharmacodynamic model which allows for mechanistic integration of antimicrobial drug effects on the cellular level to predict the impact on bacterial growth.

Methods



- Two sub-populations: Normal (n) and persisting cells (p), which switch their phenotype with rate constants μ_{np} and μ_{pn}
- Antibiotic concentration c_{drug} acts on some **death model** and some **growth model**
- Transition constant λ is predicted by some **transition model**
- Growth is limited by carrying capacity N_{max}

$$\begin{aligned} \frac{dn}{dt} &= \mu_{growth}(1 - (n+p)/N_{max})n - \mu_{death}n - \mu_{np}n + \mu_{pn}p \\ \frac{dp}{dt} &= \mu_{np}n - \mu_{pn}p \\ \frac{d\mu_{growth}}{dt} &= \lambda(\mu_{growth,adapted} - \mu_{growth}) \end{aligned}$$

Death model

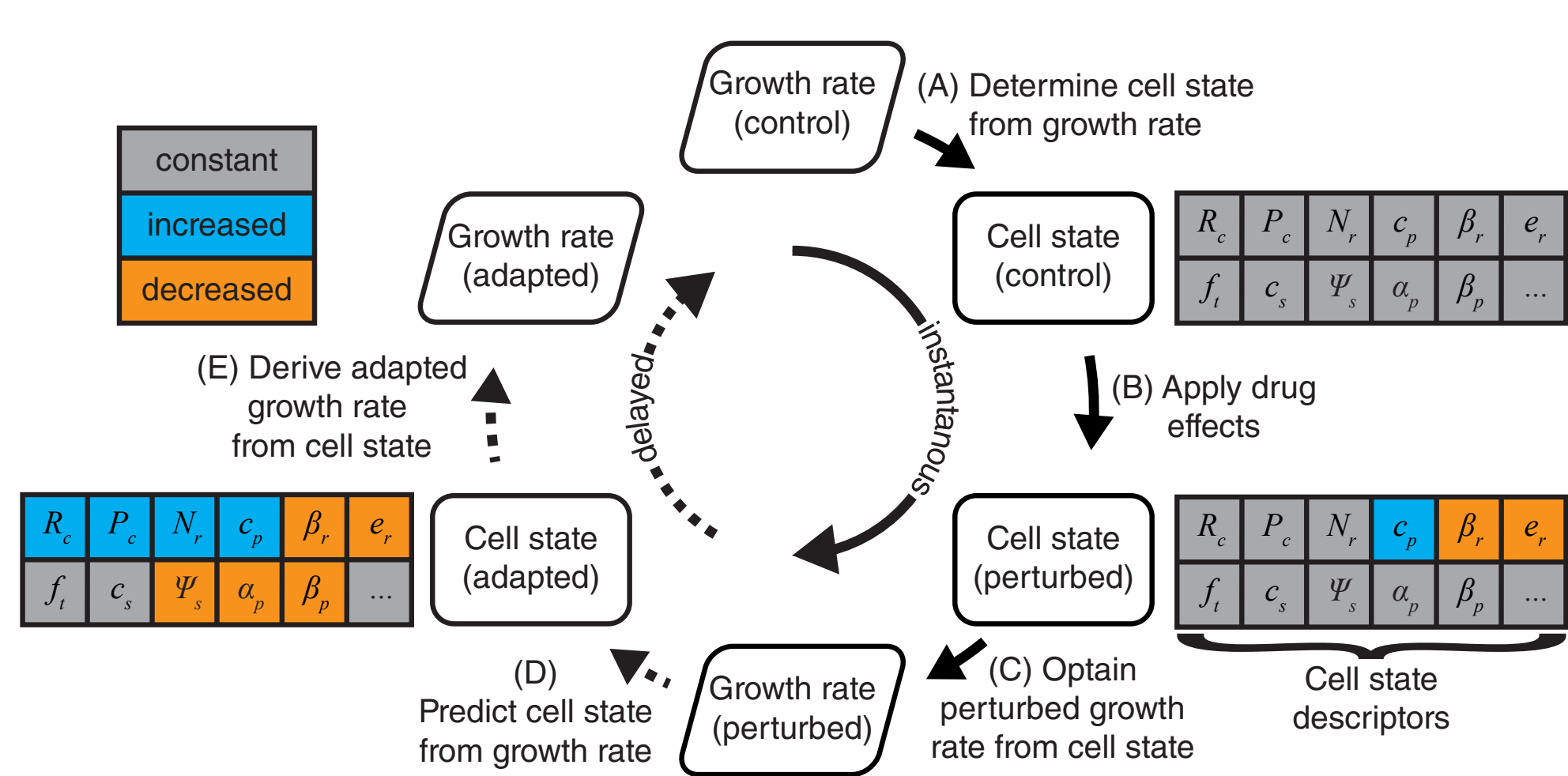
Based on data in [11], we assumed, that the baseline probability for death per cell is constant for i) all generations (no senescence) and ii) all phases of the cell cycle with $K_{death} = 0.01$.

$$\mu_{death} = K_{death} \cdot \mu_{growth,control} + \frac{E_{max,death} \cdot c_{drug}^{\gamma_{death}}}{EC_{50,death} + c_{drug}^{\gamma_{death}}}$$

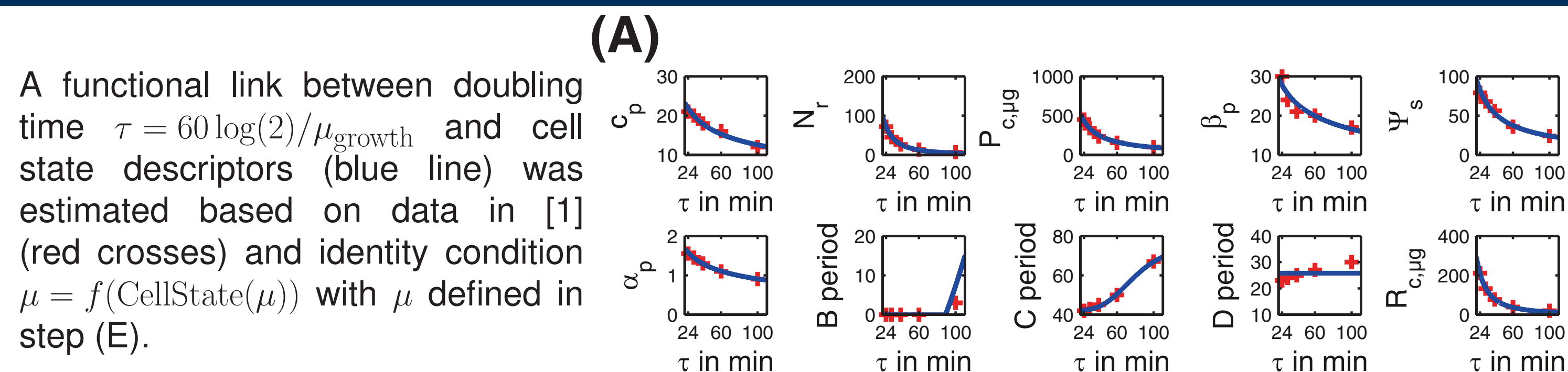
Growth model

The mechanism of action is exemplified for **protein biosynthesis inhibitors** tetracycline and chloramphenicol, which inhibit translation during the elongation phase. They share the kinetic properties of long binding times to their ribosomal targets (several minutes) — compared to the typical time a ribosome spends in the elongation phase ($\approx 280 \cdot 0.04$ s for *E. coli*).

The growth model included cell states and corresponding growth rate constants. A delay for adaptational processes was predicted by a **transition model**. The partitioning of the cell state is in accordance with a RelA and SpoT homologue regulation network (relaxed response).



Parameter abbreviations and units: β_r fraction of active ribosomes; c_p peptide chain elongation rate per active ribosome in aa/s; e_r ribosomal efficiency in aa/s ($= c_p \beta_r$); N_r number of 10^3 ribosomes per cell; $P_{c,mg}$ protein mass per 10^9 cells in μ g; $R_{c,mg}$ RNA mass per 10^9 cells in μ g; β_p fraction of active RNA polymerase in %; Ψ_s fraction of active RNA polymerase synthesizing rRNA and tRNA in %; α_p fraction of total protein that is RNA polymerase in %; M_c cell dry weight per 10^9 cells in μ g; $nucl./prib.$ ribonucleotide residues per rRNA precursor; $aa/pol.$ amino acid residues per RNA polymerase core; f_s fraction of stable RNA that is tRNA; e_s stable RNA chain elongation in $nucl/s$; $nucl./rib.$ ribonucleotide residues per 70S ribosome; f_n fraction of RNA that is stable RNA.

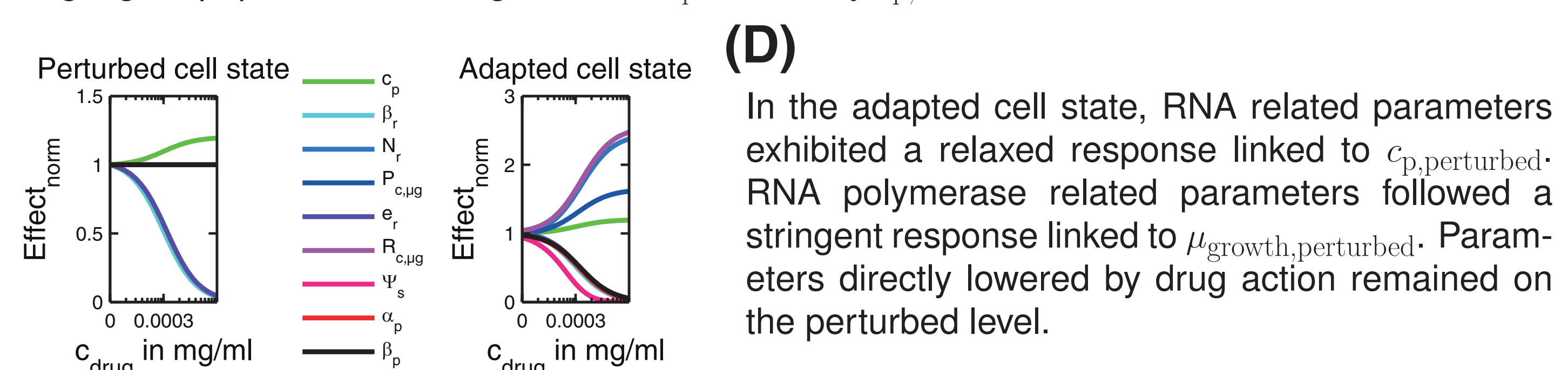


$$\beta_{r,perturbed} = \beta_{r,control} \cdot \left(1 - \frac{c_{drug}^{\gamma_{growth}}}{EC_{50,growth} + c_{drug}^{\gamma_{growth}}}\right) \quad c_{p,perturbed} = c_{p,control} + \frac{(c_{p,max} - c_{p,control}) \cdot c_{drug}^{\gamma_{growth}}}{EC_{50,growth} + c_{drug}^{\gamma_{growth}}}$$

We applied Liebig's law of the minimum by deriving the inverse of the most limiting cell state descriptor in $CellState_{perturbed}$ — for chloramphenicol and tetracycline this is the ribosomal efficiency ($e_r = \beta_r \cdot c_p$)

$$(C) \mu_{growth,perturbed} = 60 \log(2) / f_{e_r}^{-1}(e_{r,perturbed})$$

In the perturbed cell state, the fraction of active ribosomes β_r was modulated by c_{drug} with an Emax model. The remaining active ribosomes could benefit from increased amino acid pool levels and thus resulting higher peptide chain elongation rate c_p , limited by $c_{p,max}$.

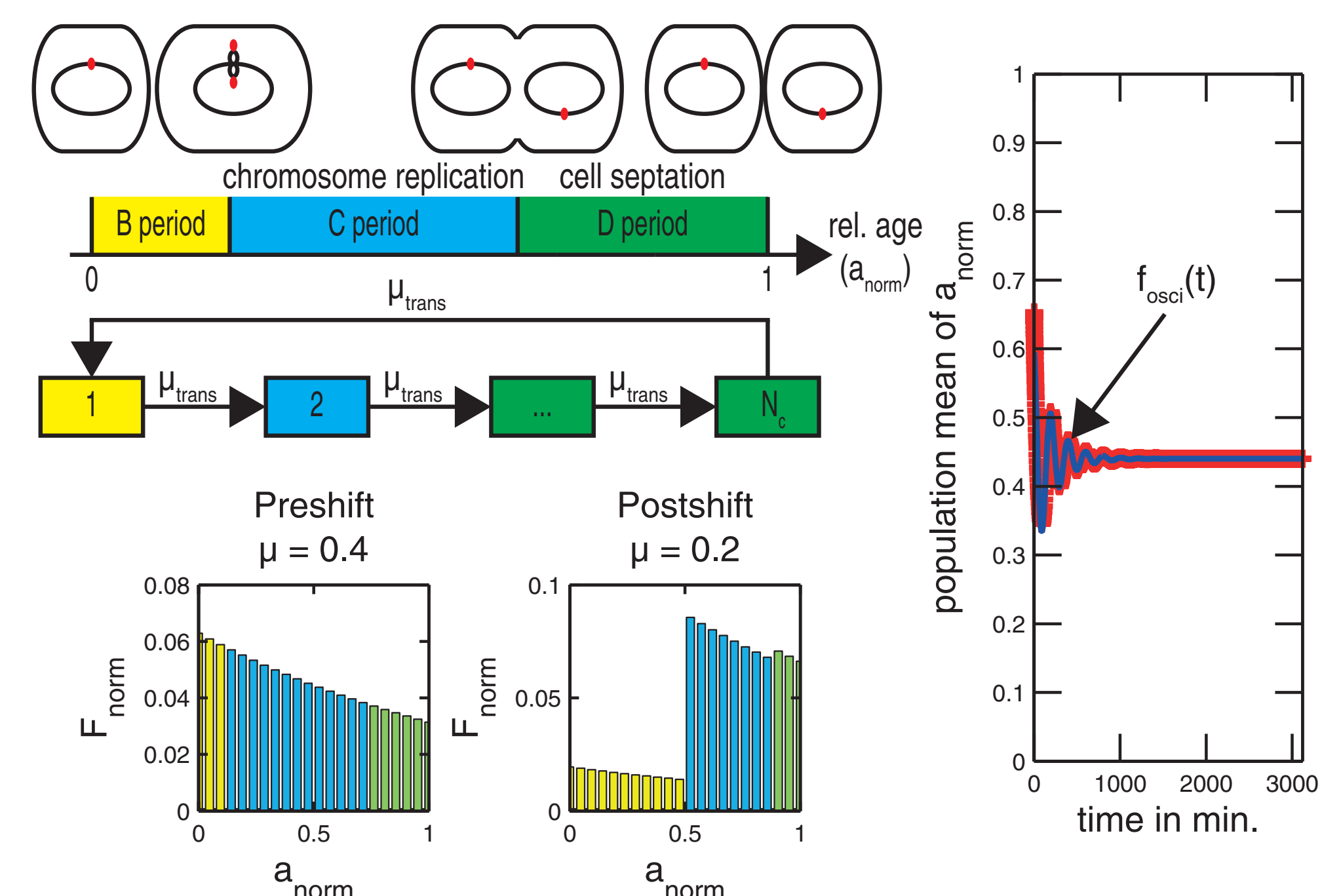


$$(E) \mu_{growth,adapted} = \frac{60}{[(nucl./prib.) \cdot (aa/pol.) / (1 - f_t)]^{0.5} (\Psi_s \alpha_p \beta_p \beta_r c_s c_p)^{0.5}}$$

Transition model

The aim is to predict the time needed for transit between pre-shift and post-shift growth rate.

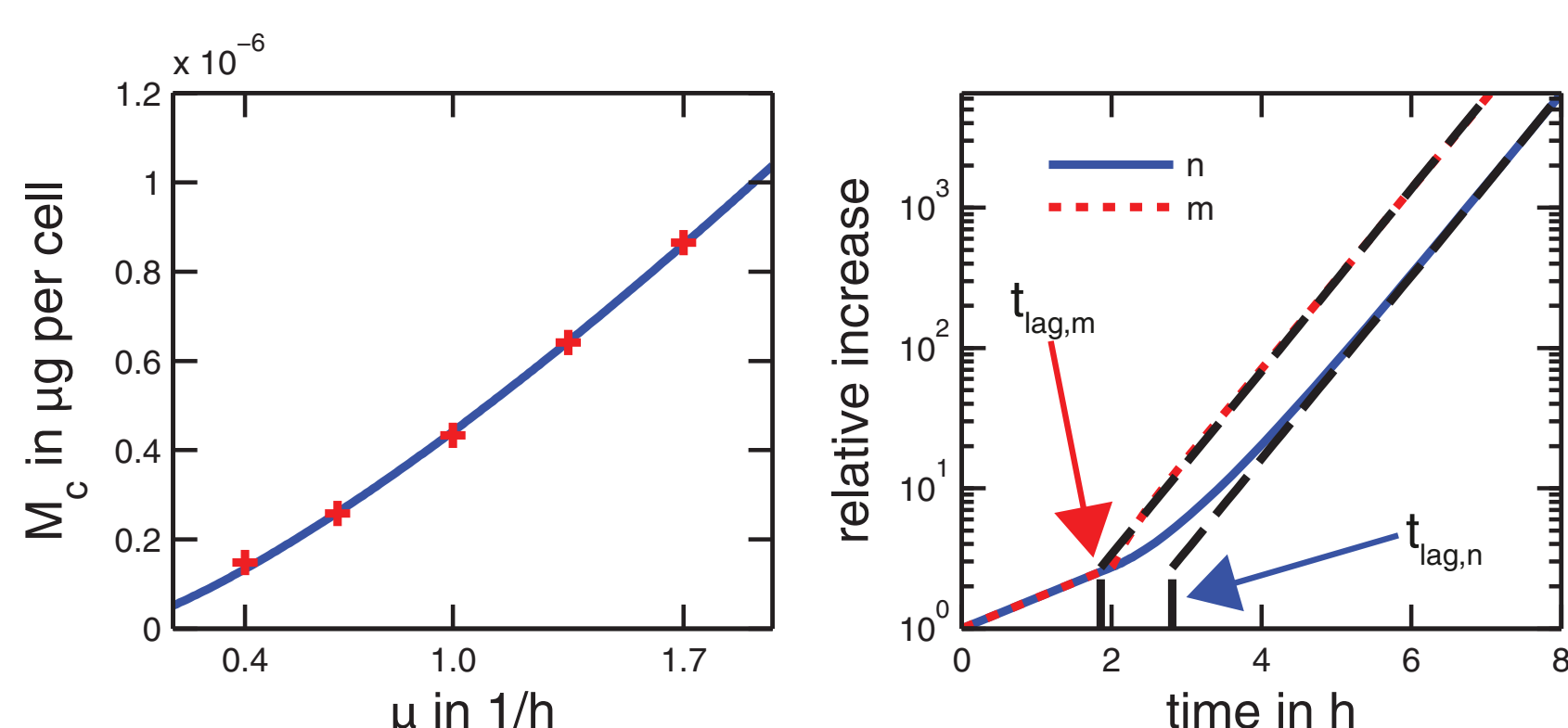
- a_{norm} describes the gradual progress of a single cell in the cell cycle and was ideally distributed with $F = 2^{1-a_{norm}}$
- A re-scaled and shifted post-shift distribution gave initial values for a transit compartment cell cycle model
- N_c and μ_{trans} was given by the known variance of the resulting Erlang distribution ($\sigma^2 = N_c / \mu_{trans}^2$)
- Decay rate of the envelope of $f_{osci}(t)$ gave transition rate constant λ



Results

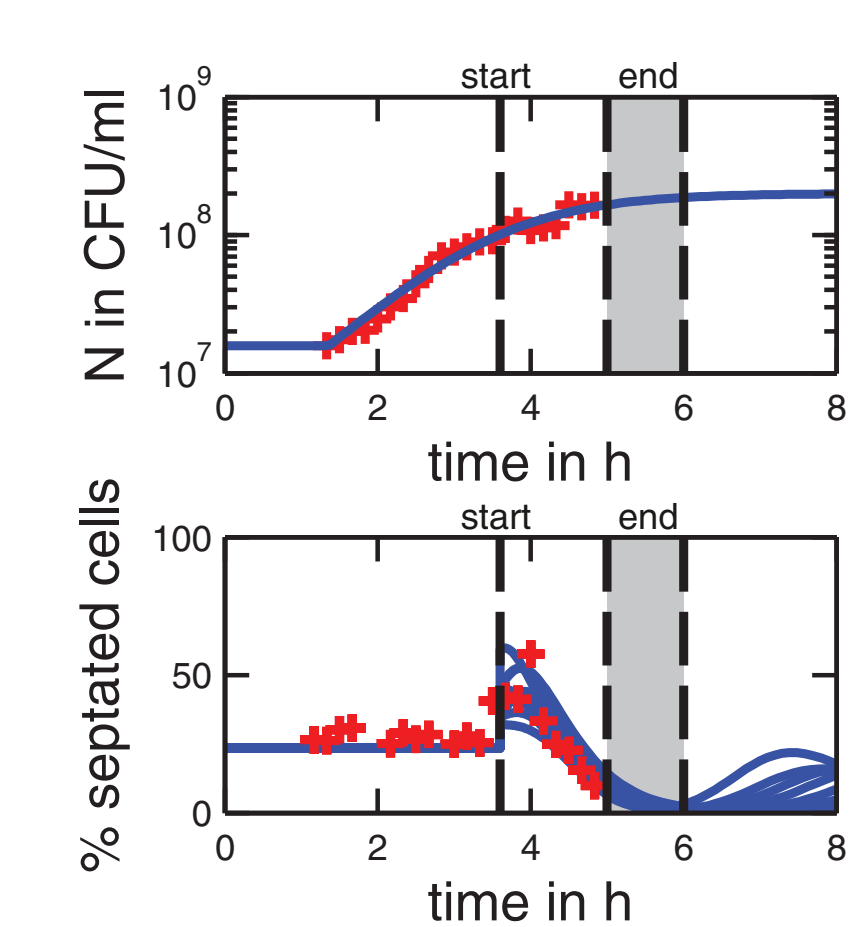
Predictions of lag between increase in cell number and population mass

In this experiment additional nutrients were added into the growth medium at $t = 2$ h. A shift-up lead to increasing mass per typical cell M_c . The transition model predicted different lag times for mass increase ($m = nM_c(\mu)$) and increase in cell number (n).



For *E. coli* B/r, with parameters estimated from data in [1] (red crosses), we can quantitatively predict $\Delta t_{lag} \approx 1$ h.

Prediction of septation dynamics of *B. subtilis*

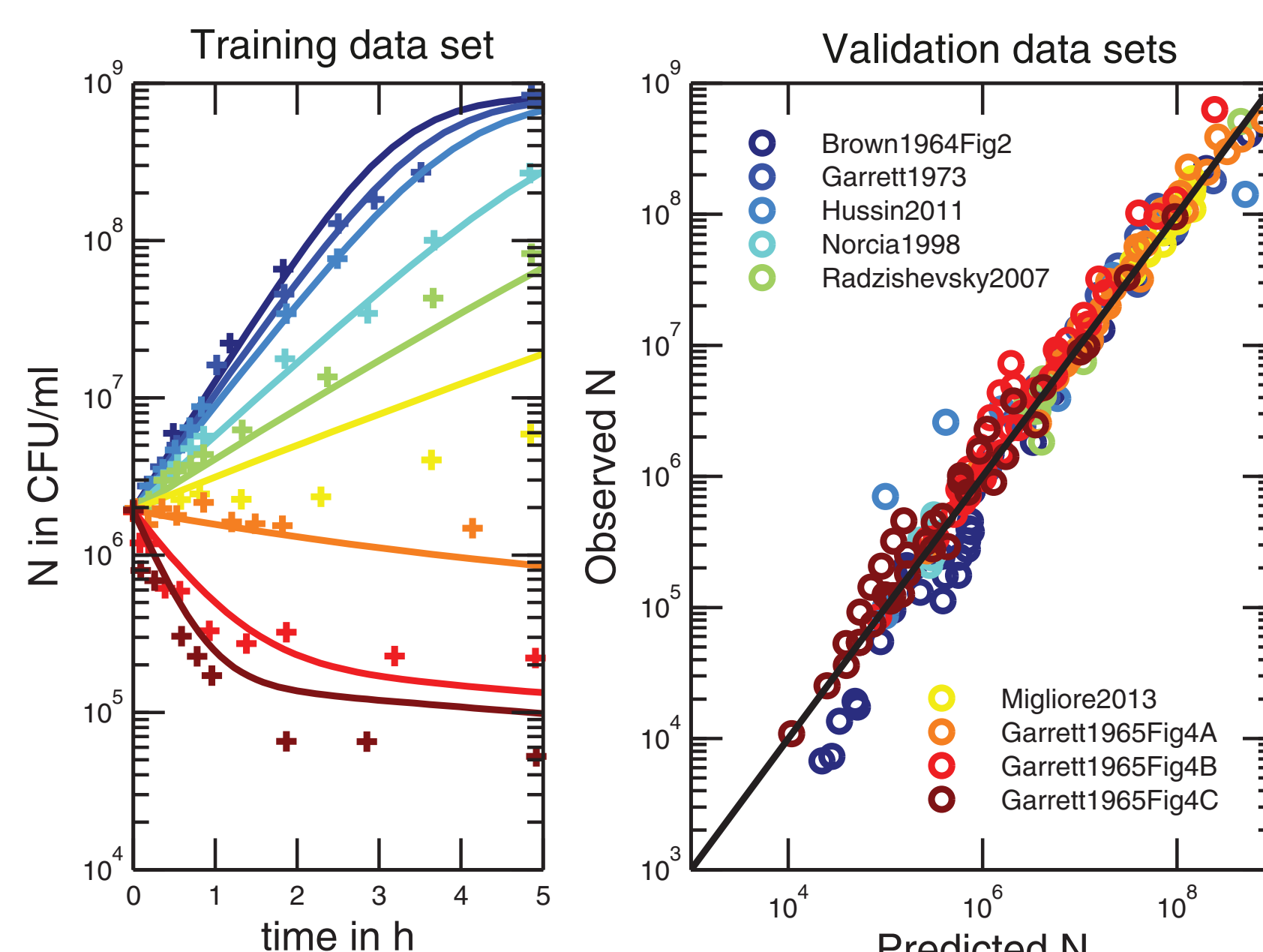


Population dynamics (N) were fitted by a logistic growth function with lag time. Its derivative gave pre- and post-shift growth rates.

- Experimental data as red crosses from [3]
 - Predictions from the transition model for 10 post-shift growth rates as blue lines
- Oscillations in age distribution faded out ≈ 4 h after start of transition.

Prediction of population dynamics for *E. coli* exposed to tetracycline

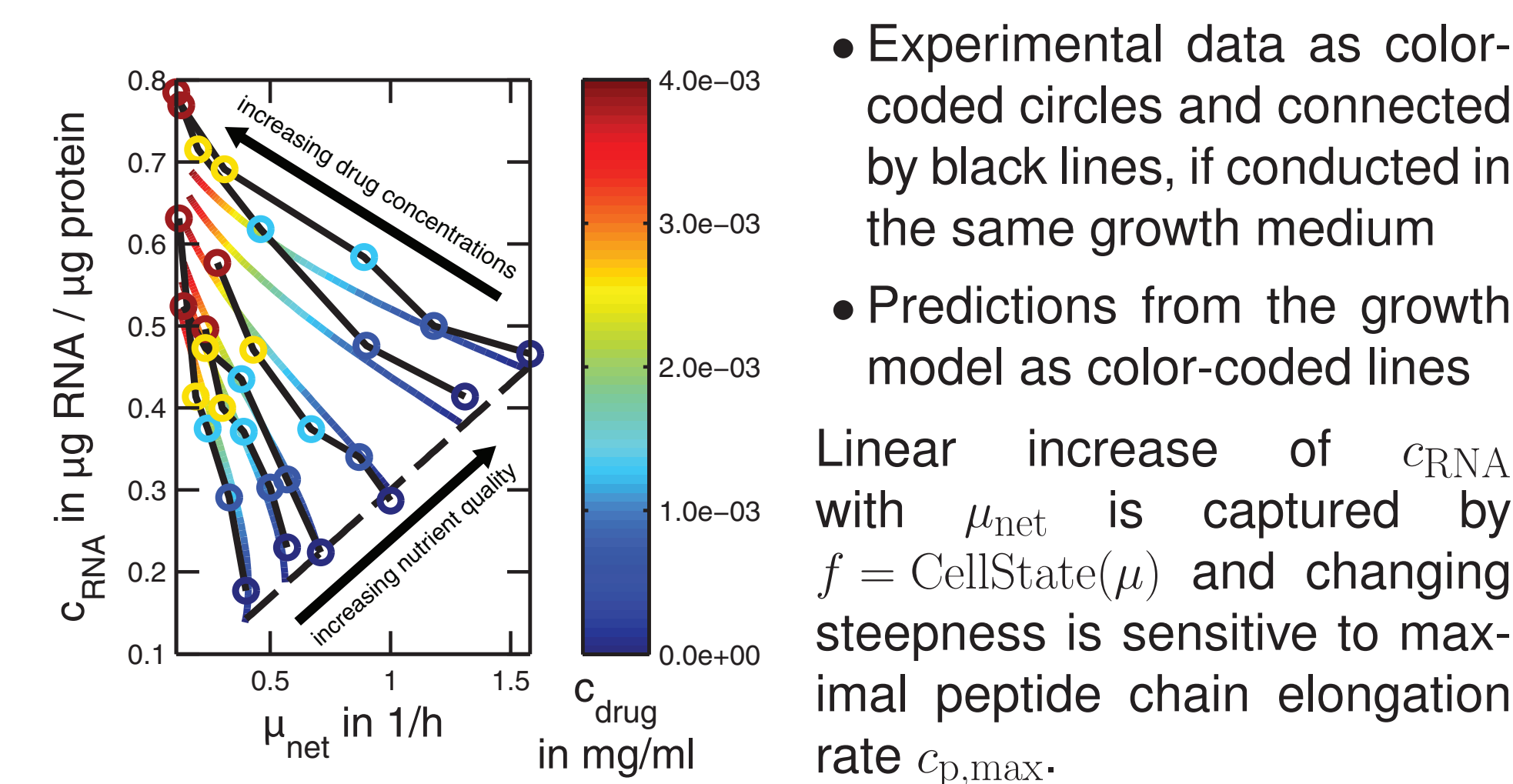
Two drug specific EC_{50} parameters were estimated in a training data set for *E. coli* B/r and static concentrations up to $8 \mu\text{g mL}^{-1}$ of tetracycline (color coded in training data set from [2]).



For validation purposes, data from different strains (B/r, ATCC 25922, ATCC 51A0150 and MG165) and growth media (Antibiotic medium 3 and Mueller Hinton) were used [2, 5, 6, 8, 9, 7, 4]. Drug specific parameters were scaled accordingly for each strain. We see very good agreement in these data sets.

Predictions of intracellular RNA concentration for *E. coli* exposed to chloramphenicol

RNA concentrations (c_{RNA}) during exponential growth were measured in several growth media and resulting growth rates μ_{net} [10]. Chloramphenicol was added in various concentrations.



- Experimental data as color-coded circles and connected by black lines, if conducted in the same growth medium
 - Predictions from the growth model as color-coded lines
- Linear increase of c_{RNA} with μ_{net} is captured by $f = CellState(\mu)$ and changing steepness is sensitive to maximal peptide chain elongation rate $c_{p,max}$.

Summary

Exploitation of cell state — growth rate interrelation enables **flexible integration of antibiotic drug effects**. Separation of system and drug specific parameters allows transfer of information between experiments. **Biological interpretation** of parameters can guide follow-up experiments and give insight into cellular responses to exposure to antibiotics.

[1] H. Bremer and P. P. Dennis. Modulation of Chemical Composition and Other Parameters of the Cell by Growth Rate. In F. C. Neidhardt, editor, *Escherichia Coli Salmonella Typhimurium Vol 2 Cell, Mol. Biol.*, number 122, chapter 96, pages 1527–1540. American Society for Microbiology, 2, edition, 1987.

[2] M. R. W. Brown and E. R. Garrett. Kinetics and Mechanisms of Action of Antibiotics on Microorganisms I - Reproducibility of *Escherichia coli* Growth Curves and Dependence Upon Tetracycline Concentration. *J. Pharm. Sci.*, 53(2):173–183, 1964.

[3] H. Funakoshi and A. Yamada. Transition Phenomena in Bacterial Growth Between Logarithmic and Stationary Phases. *J. Math. Biol.*, 9:369–387, 1980.

[4] E. R. Garrett and G. H. Miller. Kinetics and Mechanisms of Action of Antibiotics on Microorganisms III - Inhibitory Action of Tetracycline and Chloramphenicol on *Escherichia coli* Established by Total and Viable Counts. *J. Pharm. Sci.*, 54(3):427–431, Mar. 1965.

[5] E. R. Garrett and C. M. Won. Kinetics and Mechanisms of Drug Action on Microorganisms XVII: Bactericidal Effects of Penicillin, Kanamycin, and Rifampin with and without Organism Pretreatment with Bacteriostatic Chloramphenicol, Tetracycline, and Novobiocin. *J. Pharm. Sci.*, 62(10):1666–1673, 1973.

[6] W. A. Hussin and W. M. El-Sayed. Synergistic Interaction Between Selected Botanical Extracts and Tetracycline Against Gram Positive and Gram Negative Bacteria. *J. Biol. Sci.*, 11(7):433–441, 2011.

[7] L. Migliore, A. Rotini, and M. C. Thaller. Low Doses of Tetracycline Trigger the *E. coli* Growth: A Case of Homeostatic Response. *Dose-response*, 11:565–572, Jan. 2013.

[8] L. J. L. Norcia and A. M. Silvia. Studies on Time-Kill Kinetics of Different Classes of Antibiotics Against Veterinary Pathogenic Bacteria Including *Pasteurella*, *Actinobacillus* and *Escherichia coli*. *J. Antibiot. (Tokyo)*, 52(1):52–60, 1999.

[9] I. S. Radzishewsky, S. Rotem, D. Bourdetsky, S. Navon-Venezia, Y. Carmeli, and A. Mor. Improved antimicrobial peptides based on acyllysine oligomers. *Nat. Biotechnol.*, 25(6):657–9, June 2007.

[10] M. Scott, E. M. Matescus, Z. Zhang, and T. Hwa. Interdependence of Cell Growth Origins and Consequences. *Science* (80-.), 330(November):1099–1102, 2010.

[11] Y. Wang, F. Hammes, K. De Roy, W. Verstraete, and N. Boon. Past, present and future applications of flow cytometry in aquatic microbiology. *Trends Biotechnol.*, 28(8):416–24, Aug. 2010.

Contact: hethey@uni-potsdam.de